

# Surface Emitting Laser for Multimode Data Link Applications

A surface emitting laser has been developed for use in a multimode optical fiber data link. The laser can operate in a high-order spatial mode, resulting in a spectral width as wide as one nanometer and a relative intensity noise (RIN) lower than  $-125$  dB/Hz in a multimode fiber system. Electrical and optical characteristics of the surface emitting laser and the epitaxial growth methods are discussed.

by Michael R.T. Tan, Kenneth H. Hahn, Yu-Min D. Houg, and Shih-Yuan Wang

A platelet laser with light emitting perpendicular to the substrate was developed by Melngalis in 1965 at MIT Lincoln Laboratory.<sup>1</sup> By 1979, a pulsed double heterostructure InGaAsP surface emitting laser operating at cryogenic temperatures was demonstrated by Professor Suematsu's group at Tokyo Institute of Technology.<sup>2</sup> Since the late 1980s many research groups have successfully demonstrated surface emitting lasers that were electrically pumped and operating CW at room temperature.

Why are surface emitting lasers the focus of so much work? The surface emitting laser structure is radically different from the conventional edge emitting semiconductor laser. The light emitted from the surface emitting laser is perpendicular to the substrate rather than in the plane of the substrate, as shown in Fig. 1. The optical cavity of a surface emitting laser

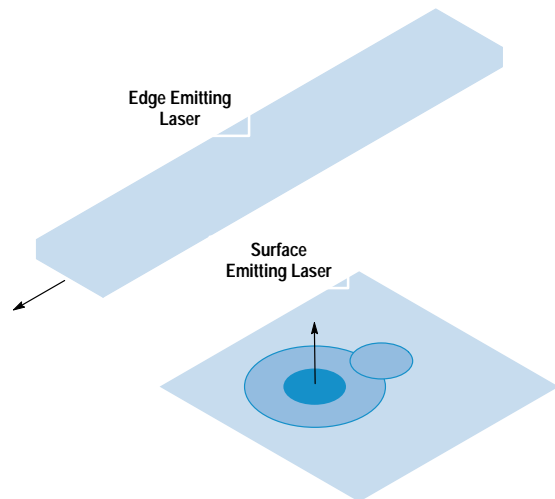


**Fig. 1.** Edge emitting lasers are cleaved into long bars typically 200 to 300  $\mu\text{m}$  long and light is emitted from the cleaved facets. Generally, it produces an elliptical beam with a numerical aperture NA of 0.3 and 0.6. The surface emitting laser emits light in a direction perpendicular to the wafer with a circular beam and an NA as small as 0.05 for a single spatial mode. This small NA simplifies interfacing to optical fibers. In addition, the surface emitting laser can be manufactured like light-emitting diodes (LED) and is complete at the wafer level.

is formed by distributed Bragg reflectors sandwiching an active layer.

Fig. 2 shows the cross section of a bottom emitting laser (light emerging from the substrate) that has been developed in our laboratory. It has a hybrid Au-Bragg "back" reflector of 99.96% reflectivity (calculated) and an output mirror of 98.9% reflectivity (calculated). This configuration is amenable to high-volume manufacturing similar to light-emitting diode (LED) processing and therefore has the potential of very low cost along with high performance.

Some advantages of the surface emitting laser over the conventional edge emitting laser are: (1) the devices are completed at the wafer level and hence can be completely characterized, (2) the numerical aperture (NA) is smaller and symmetric and allows almost 100% coupling into optical fibers, resulting in simpler packaging, (3) operation is single-frequency, and (4) the structure can be integrated with monitor photodiodes or transistors, or in two-dimensional arrays as shown in Fig. 3.

## Data Link Applications

High-speed optical data links for distances of under one kilometer for linking workstations, peripherals, and displays are becoming increasingly important. The optical source for such links has been the CD (compact disk) laser operating multimode or in the self-pulsating mode to broaden the spectrum to minimize the modal noise resulting from mode dependent loss in the multimode fiber system. Some limitations of the CD laser are that the laser has to be preselected for its self-pulsating characteristics and the modulation frequency is limited to approximately one third<sup>3</sup> of the self-pulsating frequency which is typically 1.5 to 2 GHz. A properly designed large-area surface emitting laser will not have these limitations and is an excellent light source for a multimode data link.<sup>4,5</sup>

## Growth Method

The epitaxial layers of the laser shown in Fig. 2 were grown using a modified Varian Modular Gen II molecular beam epitaxy machine. In addition to the standard high-temperature effusion cells providing the group III sources of Al, Ga, and

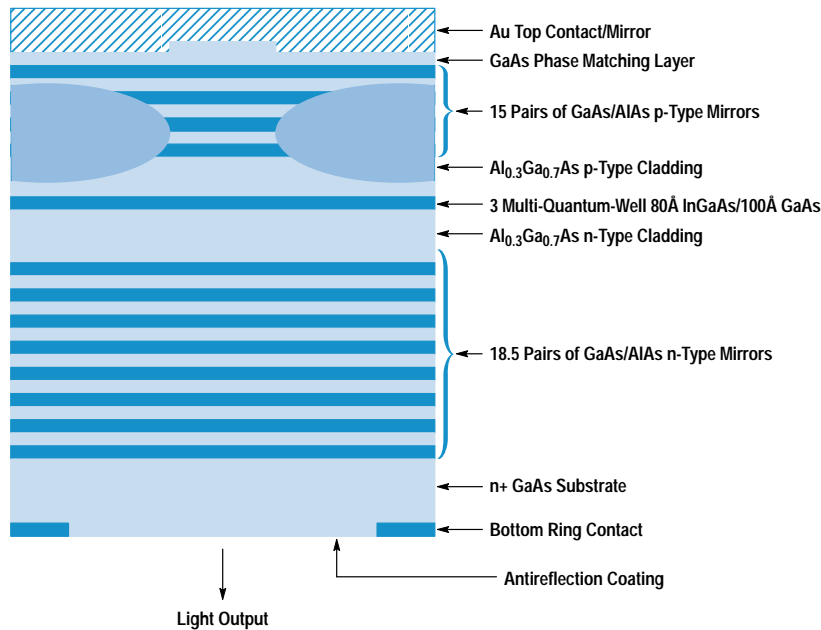


**Fig. 2.** This is a cross section of a bottom emitting laser with strained multiple quantum wells of InGaAs emitting at a wavelength of 980 nm. It has a totally reflective mirror consisting of hybrid Au/semiconductor distributed Bragg reflectors to minimize series resistivity and an output mirror consisting of semiconductor distributed Bragg reflectors. Proton ion implantation is used to confine the current.

In and the group V arsenic source  $As_4$ , the machine is also equipped with a high-temperature hydride cracker for introducing  $AsH_3$  to provide arsenic and a low-temperature gas injector for introducing the p-type dopant of carbon tetrabromide ( $CBr_4$ ). The n-type dopant used in this work was Si produced by elemental Si in a high-temperature effusion cell. The p-type dopant used is carbon. All growths were performed at 520°C on a 2-inch-diameter n+ substrate.

To maintain the alignment of the gain peak within 10 nm (blue shifted) of the Fabry-Perot wavelength, uniform control of the thickness and alloy composition must be maintained to better than 1% across the wafer. The total growth time for the bottom emitting laser structure is from 8 to 12 hours. To maintain stable growth over this time, an in-situ growth-monitoring technique using a pyrometer is used.<sup>6,7,8</sup> During the growth of the Bragg mirrors consisting of quarter-wavelength thicknesses of GaAs and AlAs, the emission intensity from the heated wafer is detected by a pyrometer. The signal is oscillatory in nature and is directly correlated with the growth of the alternating Bragg layers. Fig. 4 shows the run-to-run reproducibility using the in-situ monitoring technique, the Fabry-Perot wavelength can be achieved within  $\pm 1\%$  for several different runs.

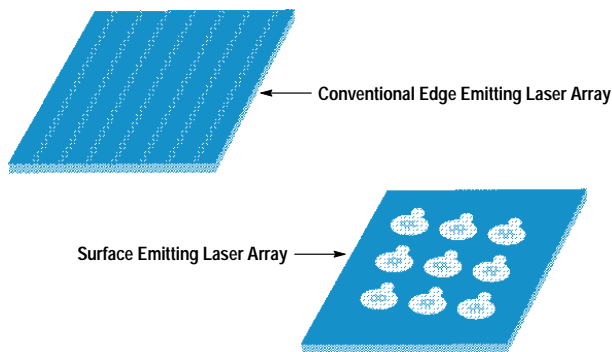


**Fig. 3.** Surface emitting lasers can be made into two-dimensional arrays and integrated with monitor photodiodes. It is much more difficult to accomplish these things in the edge emitting laser.

### Device Design

The surface emitting laser is a bottom emitting structure with strained InGaAs quantum wells emitting at 980 nm. As shown in Fig. 2, it consists of 18.5 pairs of n-type GaAs and AlAs Bragg mirrors on the output face and 15 pairs of p-type GaAs and AlAs together with an Au mirror on the totally reflective face. The cavity is a single wavelength wide and consists of an active region of three 80-angstrom strained InGaAs quantum wells with 100-angstrom GaAs barriers and about 970 angstroms of  $Al_{0.3}Ga_{0.7}As$  carrier-confining layers. The interface between GaAs and AlAs in the distributed Bragg reflector mirrors is digitally graded in eight steps using a chirped short-period superlattice. The final p-type GaAs phase-matching layer is doped to  $3 \times 10^{19}/cm^3$  to provide a nonalloyed ohmic contact to the hybrid Au mirror, which also acts as a p contact. The GaAs and AlAs Bragg mirrors

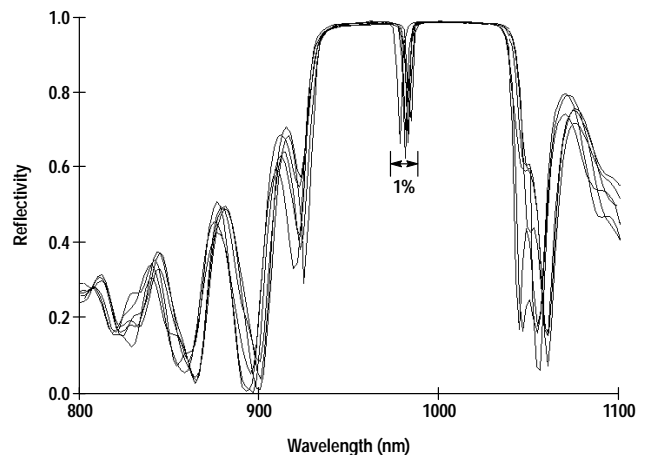
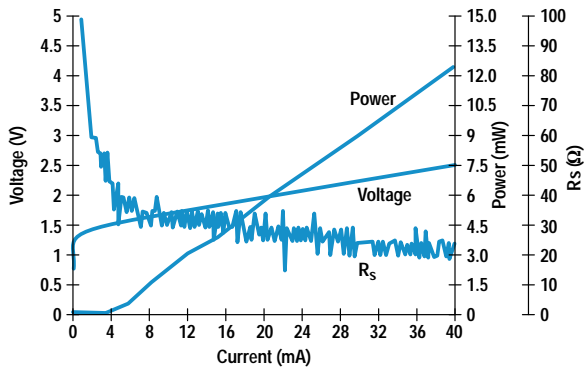


**Fig. 4.** The stop band characteristics (reflectivity versus wavelength plots) of six different epitaxial runs demonstrate the run-to-run reproducibility achieved with in-situ growth monitoring. The dip in the stop band is caused by the Fabry-Perot cavity formed by the two distributed Bragg reflector mirrors. Variation of the Fabry-Perot wavelength can be kept under 1%. The reflectometer is calibrated by the water vapor absorption line at 942 nm.



Typical Characteristics	
$R_s$	$\sim 20\Omega$
$V_{th}$	1.40V
$I_{th}$	3.8 mA
$P_o$	$>12$ mW
$\eta_{ext}$	$\sim 27\%$
$f_{3dB}$	$\sim 6$ GHz
$Z_{th}$	$176^\circ\text{C/W}$

**Fig. 5.** Dc characteristics of a large-area 980-nm surface emitting laser. The curves show voltage, optical power output, and series resistance as a function of bias current. The table shows typical parameters obtained for such surface emitting lasers.

are uniformly doped to  $1 \times 10^{18}/\text{cm}^3$  except for the digital grading region which is uniformly doped to  $5 \times 10^{18}/\text{cm}^3$ . The n dopant is Si and the p dopant is carbon which has been shown not to diffuse<sup>6,7</sup> out of the graded region.

### Fabrication Steps and Device Characteristics

The basic fabrication steps for the bottom emitting laser are as follows. When the wafer is received from the grower of the epitaxial layers, its reflectivity is measured in a spectrophotometer to determine the stop band and the wavelength of the Fabry-Perot cavity. A small piece of the wafer is fabricated into a broad-area laser to determine the threshold current and the peak-gain wavelength. The Fabry-Perot wavelength and the peak-gain wavelength are important parameters for the surface emitting laser. Ideally, we would like the peak-gain wavelength to be blue-shifted by 10 nm with respect to the Fabry-Perot wavelength.

Next, the rest of the wafer is coated with gold film in an evaporator. The gold serves as a mirror in addition to the Bragg mirror, further boosting the reflectivity of the end mirror. A photoresist ion implant mask is then defined and the gold field is chemically removed. Protons of varying energy and dosage are implanted to confine the current. Photolithography is then used again to define a gold plating for die attachment. After gold plating, the wafer is lapped and polished to an accuracy of 0.005 inch. Finally, ohmic contacts

and antireflection coatings are deposited, their areas defined by photolithography. This completes the surface emitting laser.

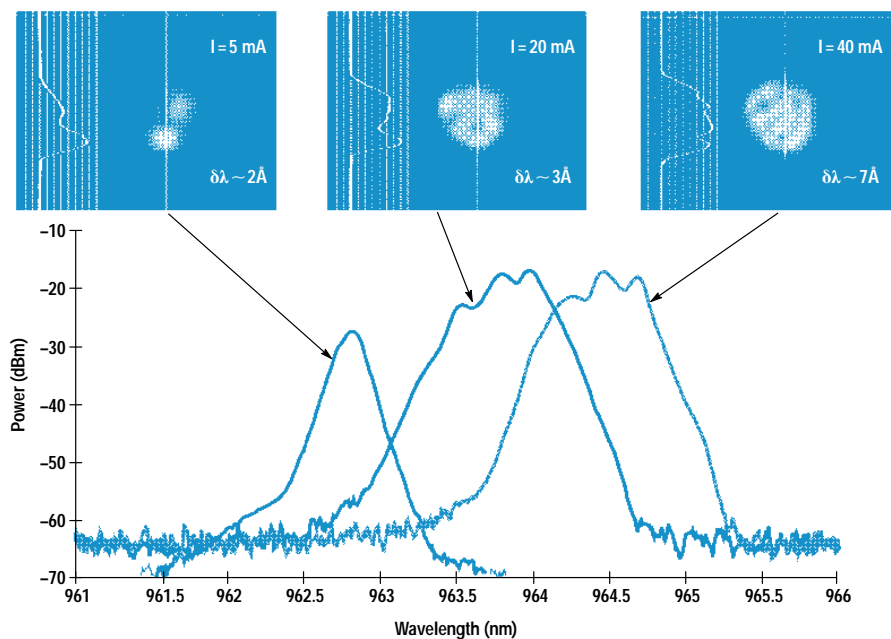
Surface emitting lasers with 24- $\mu\text{m}$  active diameters have turn-on voltages as low as 1.40V and threshold current of 3.0 mA. Wallplug efficiencies<sup>†</sup> of 13% have been demonstrated. The I-V and L-I (light power output versus current) curves of the laser are shown in Fig. 5. The kinks in the L-I curve are from filamentation or higher-order spatial modes appearing in the laser cavity as the bias is increased. The 1.40V turn-on voltage is only 0.28V above the InGaAs bandgap energy. The series resistance of the device is 20 ohms.

### Spectral Width

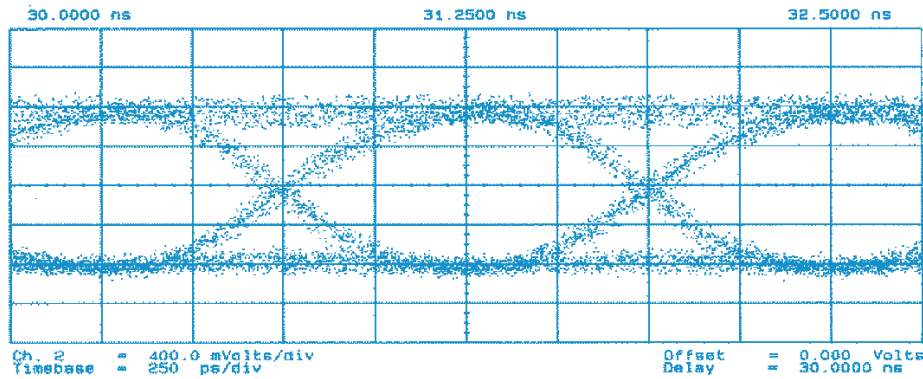
A wide spectral width is necessary to reduce the effect of modal noise resulting from mode-selective loss in multimode links. The surface emitting laser with an active width of 24  $\mu\text{m}$  was found to give a spectral width of 0.3 to 0.7 nm. The wide active region is necessary to allow the accommodation of multiple filaments or higher-order modes whose simultaneous existence gives rise to the wide spectral width.

Fig. 6 shows the near-field pattern of the surface emitting laser and the associated spectrum as a function of the bias. As the bias is increased from 5 mA to 40 mA, the spectrum

<sup>†</sup> Wallplug efficiency is optical power out divided by electrical power in.



**Fig. 6.** A primary characteristic of the large-area surface emitting laser is its broad linewidth, which is important to minimize modal noise when using multimode optical fibers. This figure shows the near-field pattern and the associated spectrum as a function of bias current. The broad spectrum is a result of the increased number of spatial modes and the formation of multifilaments, each emitting at a slightly different frequency.



**Fig. 7.** The large-area surface emitting laser modulated at 1 Gbit/s using a  $2^7-1$  pseudorandom bit sequence exhibits a clean eye diagram. The laser is prebiased at 27.8 mA and a large modulation signal is applied. The modulated signal is detected after traversing a length of multimode fiber.

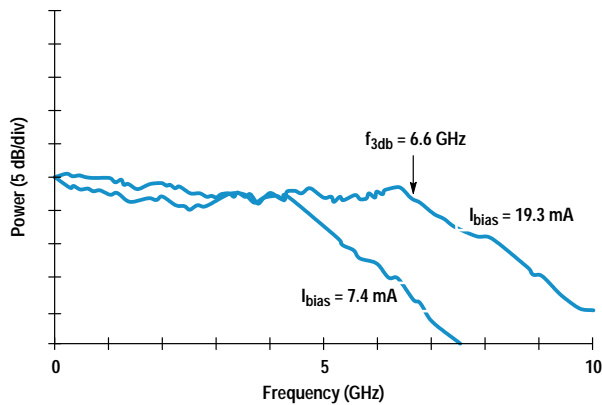


**Fig. 8.** This power-versus-modulation-frequency plot shows a 3-dB bandwidth of 6.6 GHz under small-signal modulation. The curve with the higher bandwidth corresponds to a bias current of 10.3 mA and the curve with the lower bandwidth corresponds to a bias current of 7.4 mA.

broadens from 0.2 nm to 0.7 nm. Fig. 7 shows the eye diagram at one Gbit/s modulation with the surface emitting laser biased at 27.8 mA using a  $2^7-1$  pseudorandom bit sequence. A bit error rate (BER) of better than  $10^{-12}$  at 1 Gbit/s, good eye opening, and low modal and intensity noise have been obtained with these devices.

The small-signal frequency response of the surface emitting laser is shown in Fig. 8. The useful bandwidth is greater than 6 GHz.

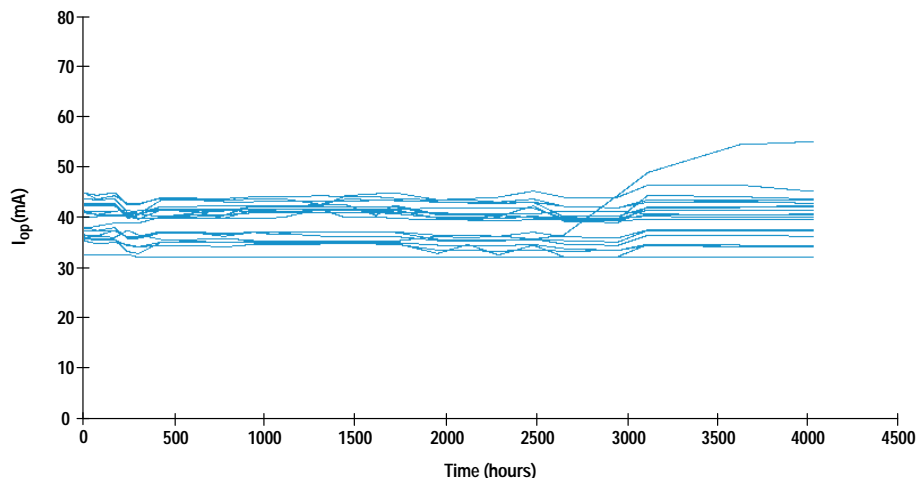


**Fig. 9.** The surface emitting laser is currently undergoing constant-power life testing. This figure is for 20 preselected lasers operating at 60°C ambient temperature at a light output power of 1 mW. The vertical axis is the current to maintain 1-mW output power and the horizontal axis is the test time in hours.

### Reliability

The major burn-in failure that we have observed is that of dark line defects and dark spot defects. The burn-in screening investigation showed that a short constant-current stress is effective in screening out early failures. The conditions used for the burn-in are 70°C and  $10^4$  A/cm<sup>2</sup> for 24 hours. The devices that pass the burn-in screening are stressed at 60°C at 1 mW and have lived over 4000 hours at the time of writing of this paper. Fig. 9 shows the light output power of 1 mW at 60°C as a function of time.

### Conclusion

Large-area surface emitting lasers with wide linewidths are good candidates as sources for short-distance high-speed links using multimode fibers. These surface emitting lasers can replace self-pulsating CD lasers and offer higher bandwidths than the CD lasers.

### Acknowledgments

A close collaboration was formed with the HP Optical Communication Division (OCD) to study the reliability of the surface emitting laser. The OCD team was led by Al Yuen and consisted of Tao Zhang, Chun Lei, Christa Tomasevich, Helen Crusco, and Jay Bhagat. The reliability results presented in this paper are the fruits of the joint effort of OCD and HP Laboratories. The authors also thank Long Yang for early contributions, Jean Norman for packaging, and Andreas Weber for discussions. We thank Lynette Martinez and Henrietta Gamino for device processing and Midori

Kanemura for assistance in epitaxial growth. We are grateful to Waguih Ishak, Ron Moon, Bob Weismann, Kent Carey, Jeff Miller, David Dolfi, and Andy Liao for their support of this work. Discussions on systems applications with David Cunningham that helped launch this project are also gratefully acknowledged by S.Y. Wang.

### References

1. I. Melngalis, "Longitudinal Injection Plasma Laser of InSb," *Applied Physics Letters*, Vol. 6, 1965, p. 59.
2. H. Soda, K. Iga, C. Kitahara, and Y. Suematsu, "GaInAsP/InP Surface Emitting Injection Lasers," *Japanese Journal of Applied Physics*, Vol. 18, 1979, pp 23-29.
3. D. Sears, Hewlett-Packard Optoelectronics Division, *private communication*.
4. K.H. Hahn, M.R.T. Tan, Y.M. Houng, and S.Y. Wang, "Large-Area Multitransverse Mode VCSELs for Modal Noise Reduction in Multimode Fibre Systems," *Electronics Letters*, Vol. 29, 1993, p.1482.
5. K.H. Hahn, M.R.T. Tan, and S.Y. Wang, "Intensity Noise of Large-Area Vertical-Cavity Surface Emitting Lasers in Multimode Optical Fibre Links," *Electronics Letters*, Vol. 30, 1994, p. 139.
6. Y.M. Houng, S.D. Lester, D.E. Mars, and J.N. Miller, "Growth of High-Quality p-Type GaAs Epitaxial Layers Using Carbon Tetrabromide by Gas Source Molecular Beam Epitaxy and Molecular Beam Epitaxy," *Journal of Vacuum Science and Technology*, Vol. B11, no. 3, 1993, p. 915.
7. Y.M. Houng, B.J. Lee, T.S. Low, and J.N. Miller, "Growth of High-Quality AlGaAs/GaAs Heterostructures by Gas Source Molecular Beam Epitaxy," *Journal of Vacuum Science and Technology*, Vol. B8, no. 2, 1990, p. 355.
8. Y.M. Houng, M.R.T. Tan, B.W. Liang, S.Y. Wang, and D.E. Mars, "In-Situ Thickness Monitoring and Control for Highly Reproducible Growth of Distributed Bragg Reflectors," *Journal of Vacuum Science and Technology*, Vol. B12, no. 2, 1994, p. 1221.